Ln(III) complexes as potential phosphors for white LEDs

Akerboom, S.

3 Ln(III) complexes with small aromatic ligands

In this chapter, the synthesis of four new Ln(III) complexes (Ln = Eu, Tb) with furan-2,5-dicarboxylic acid (H_2fda) as a ligand, as well as the preparation of a metal organic framework of Tb(III) with 2-hydroxytrimesic acid (H_4tma) is described. The compounds have been synthesized and characterized in the solid state. Luminescence studies indicate that the compounds exhibit line-like luminescence characteristic of the lanthanoid ion upon excitation in the ligand absorption bands. Single crystal X-ray diffraction study of $([Eu(fda)(H_2O)_5]\cdot\frac{1}{2}(fda)\cdot 3H_2O)_n$ shows the formation of an inorganic polymer with infinite Eu-FDA chains. The structure of the metal organic framework of Tb(III) with H_4tma is described by the formula $[Tb(Htma)(H_2O)_2]$ and shows emission lines characteristic for Tb(III) when excited with near-UV radiation with a quantum yield of 67%, indicating that the ligand is acting as a highly efficient antenna for sensitizing Tb(III) emission.

(Parts of this chapter have been published:
S. Akerboom, W.T. Fu, M. Lutz and E. Bouwman, *Inorg. Chim. Acta* 387 (2012) 289; S. Akerboom, X. Liu, S.H.C. Askes, I. Mutikainen, W.T. Fu, E. Bouwman, manuscript submitted)

3.1 Introduction

As discussed in the first chapter of this thesis, LED-based solid state light sources have the potential to save substantial amounts of energy and reduce CO_2 emissions. For the approach relying on (partial) conversion of the emission of a blue or nUV emitting LED, phosphor materials are required [1, 2]. The phosphor materials that are currently applied in lighting technology are not suitable, as they cannot be efficiently excited by radiation in that spectral region [3-5]. Thus, new luminescent materials are needed, and complexes of the trivalent lanthanoid ions are promising candidates. As discovered in 1942 by Weissman, the ligands in these compounds can act as an antenna that absorbs incoming radiation and transfers it subsequently to the lanthanoid ion [6]. The favorable luminescent characteristics of the lanthanoids, such as millisecond lifetime and line like emission are, therefore, retained in these compounds [7]. Unlike the oxide-based phosphors, the preparation of complexes can be carried out at much lower temperatures, usually less than 200 °C. This can significantly reduce the production costs. In addition, complexes are molecule-based solid materials. They do not require highly pure rare earths as starting materials. Furthermore, recycling the expensive rare earths can be easily achieved from complexes, e.g. by dissolution in inorganic acids or by burning. Besides these advantages, the absorption properties of complexes can be, in principle, designed to match the excitation source by modifying the ligands. Ligands that are known to be good antennae for the lanthanoid ions are β-diketonates [8-10], Schiff bases [11, 12], macrocycles [13, 14] and aromatic carboxylates [15-17]. Recent work in our group has shown that pyridine-2,6-dicarboxamide is able to sensitize both Eu^{3+} and Tb^{3+} centered luminescence efficiently [18]. In subsequent work, it was found that the structurally similar pyridine-2,6-dicarboxylate is a suitable antenna for both Eu^{3+} and Tb^{3+} complexes with quantum yields as high as 72% and 68% respectively [19]. To continue on this line of research, the present study focuses on the structurally closely related furan-2,5-dicarboxylate (H_2fda) and 2-hydroxytrimesic acid (H_4tma) ligands as antennae for europium(III) and terbium(III).

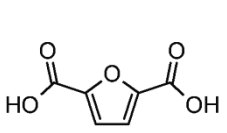

H_2fda

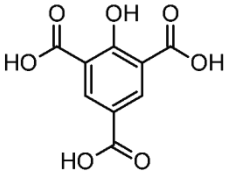

H_4tma

Ligand	Complex
H_2fda	Eufda1
	Tbfda1
	Eufda2
	Tbfda2
H_4tma	TbHtma

Figure 3.1: Overview of the ligands and complexes discussed in this chapter.

3.2 Experimental

3.2.1 General

Furan-2,5-dicarboxylic acid was purchased from Alfa-Aesar and was used as received. All other chemicals were purchased from Acros and used as-received. Pressure reaction vessels were purchased from Jinan Henghua Science & Technology Co., Ltd. To record NMR spectra, a Bruker DPX-300 spectrometer was used. Elemental analysis for C, H and N was performed on a Perkin-Elmer Paragon 2400 series II analyzer. Infrared spectra were recorded on a Perkin-Elmer Spectrum Two FTIR spectrometer equipped with the UATR Two accessory. Photoluminescence quantum yields were determined using the absolute method and an integrating sphere, following a modification of the procedure reported by de Mello et al. [20]. The integrating sphere (custom-made, based on the AvaSphere 30REFL) was connected to an irradiance calibrated CCD spectrometer (Avantes AvaSpec-2048UA). A 1000 Watt Xe-discharge lamp and a Spex monochromator were used as the excitation source. A Shimadzu RF-5301PC spectrofluoriphotometer was used to record excitation- and emission spectra. Luminescence lifetime was determined using an Edinburgh Instruments FLS920 spectrophotometer, using a pulsed laser as the excitation source. Stock solutions of europium chloride and terbium chloride were prepared by dissolving carefully weighed quantities of their respective oxides in a hot concentrated HCl solution followed by evaporation to dryness. The solids thus produced were dissolved in distilled water to yield 0.1 M solutions.

3.2.2 X-ray crystal structure determination

For **Eufda2** X-ray intensities were measured on a Bruker Kappa ApexII diffractometer with sealed tube and Triumph monochromator (λ = 0.71073 Å) up to a resolution of $(\sin\theta/\lambda)_{max}$ = 0.61 $Å^{-1}$ at a temperature of 150(2) K. The reflection profiles indicated a high mosaicity. Intensity integration was performed with the SAINT software [21]. An absorption correction based on multiple measured reflections was performed with SADABS [22] (0.56-0.75 correction range). The structure was solved with automated Patterson methods using the program DIRDIF [23] and refined with SHELXL-97 [24] against F^2 of all reflections. Hydrogen atoms were located in difference Fourier maps (hydrogen positions at O5W and O6W unreliable). C-H hydrogen atoms were refined with a riding model, O-H hydrogen atoms were kept fixed at their located positions. Geometry calculations and checking for higher symmetry was performed with the PLATON program [25]. For **TbHtma**, a crystal was selected for the X-ray measurements and mounted to the glass fiber using the oil drop method and data were collected at 173 K on a Nonius Kappa CCD diffractometer (Mo-Kα radiation, graphite monochromator, λ = 0.71073 Å) [26]. The intensity data were corrected for Lorentz and polarization effects, and for absorption. The programs COLLECT, SHELXS–97, SHELXL–97 were used for data reduction, structure

solution and structure refinement, respectively [24, 27, 28]. The nonhydrogen atoms were refined anisotropically. The hydrogen atoms were determined at the difference map and refined isotropically riding with the heavy atom connected except O2 hydrogen and water O8 hydrogens, which were refined isotropically. Further details on the crystal structure determination of **Eufda2** and **TbHtma** are given in Table 3.1.

3.2.3 Synthesis

2-hydroxy-trimesic acid (H_4tma)

Following literature procedures, 4-methylphenol (29 mmol, 3.0 g) was converted into 2-methoxy-trimesic acid [29-32]. Subsequently, this compound was converted into 2-hydroxy-trimesic acid by refluxing in 100 mL of 33% HBr in acetic acid for 120 minutes. The hot mixture was poured onto ice, after which the compound precipitated as a white microcrystalline solid. This was filtrated and dried in vacuo at 50 °C to give 2.7 g (12 mmol) of product in an overall yield of 43% based on 4-methyl-phenol. ^{1}H NMR (300 MHz, D_2O): δ 8.48 (s, 2H, H_{ar}), 8.04 (s, broad, 1H, OH). ^{13}C NMR (75 MHz, D_2O): δ 169.20 (-**C**OOH), 168.10 (-**C**OOH), 166.31 (**C**-OH), 136.85 (**C**-H), 118.12 (**C**-CO_2H), 117.44 (**C**-CO_2H). IR (ν, cm^{-1}): 2850(w, br), 1701(m), 1659(m), 1595(m), 1477(m), 1395(s), 1308(m), 1262(s), 1232(s), 1176(s), 1262(s), 1231(s), 1117(m), 891(m), 815(s), 767(m), 693(s), 652(m).

*$(H_2NMe_2)_5Ln_4Cl_3(fda)_7$ (Ln = Eu: **Eufda1**, Ln = Tb: **Tbfda1**)*

General procedure: 0.5 mmol of $LnCl_3{\cdot}xH_2O$, obtained by evaporation of 5 mL of the stock solutions, was dissolved in 10 mL of dmf. Next, 1.5 mmol of furan-2,5-dicarboxylic acid was added to this solution, which was then heated to reflux for 60 minutes. The suspension was cooled down to room temperature and the precipitates were collected by filtration and washed with ethanol. After drying the compounds were obtained in a yield of 59% (*Ln* = Eu) and 64% (*Ln* = Tb) as microcrystalline solids.

*$(H_2NMe_2)_5Eu_4Cl_3(fda)_7$ (**Eufda1**)*

Elemental analysis calculated for $C_{52}H_{54}Cl_3Eu_4N_5O_{35}$ (%): C 30.87, H 2.69, N 3.46, found (%) C 30.62, H 2.70, N 3.57. IR (ν/cm^{-1}): 1628(m), 1576(vs), 1539(s), 1362(vs), 1224(w), 1104(w), 1016(w), 780(vs), 676(m), 618(m), 494(s), 374(m).

*$(H2NMe_2)_6Tb_4Cl_4(fda)_7{\cdot}3H_2O$ (**Tbfda1**)*

Elemental analysis calculated for $C_{54}H_{60}Cl_3Tb_4N_5O_{38}$ (%): C 29.67, H 2.87, N 3.33, found (%) C 29.63, H 2.80, N 3.24. IR (ν/cm^{-1}): 1628(m), 1576(vs), 1538(s), 1362(vs), 1226(w), 1104(w), 1016(w), 780(vs), 678(m), 618(m), 496(s), 378(m).

$([Ln(fda)\cdot(H_2O)_5]\cdot\frac{1}{2}(fda)\cdot 3H_2O)_n$ (Ln = Eu: ***Eufda2****, Ln = Tb:* ***Tbfda2)***

In order to grow single crystals of $(H_2NMe_2)_6Ln_4Cl_4(fda)_7$, an attempt was made to recrystallize the solid. The compounds are insoluble in most common solvents such ethanol, methanol, chloroform, acetone, but are sparingly soluble in boiling water. **Eufda1** and **Tbfda1** were dissolved in the minimum amount of boiling water to yield clear solutions, which were slowly cooled to room temperature. The flasks with the solutions were then stored at 4 °C for several weeks, which resulted in the formation of colorless needle shaped crystals.

Eufda2 IR (ν/cm^{-1}): 3898(w, br), 1558(s), 1344(s), 1224(m), 1018(m), 966(m), 822(m), 778(s), 486(s). **Tbfda2** IR (ν_{max}/cm^{-1}): 3235(w, br), 1558(s), 1354(s), 1228(m), 1020(m), 968(m), 832(m), 782(m), 470(m).

$[Tb(Htma)(H_2O)_2]$ ***TbHtma***

A 20 mL teflon lined stainless steel pressure vessel was charged with 37 mg $TbCl_3\cdot 5H_2O$ (0.1 mmol), 67.8 mg (0.3 mmol) of H_4fda and 10 mL of demineralized water. The vessel was buried in a sand bath holding 14 kg of sand, which was then placed in an oven. The reaction mixture was reacted at 160 °C under autogenous pressure for three days. Then, the vessel was cooled down to 100 °C at a rate of 5 °C per hour, and to room temperature by natural cooling of the sand bath. The pale yellow crystals were filtered and washed with water and ethanol. Yield: 20 mg, 52% based on Tb(III). IR (ν/cm^{-1}): 3484(w, br), 1630(m), 1582(s), 1523(s), 1424(s), 1367(s), 1280(s), 1116(w), 838(w), 827(w), 787(s), 702(s), 560(s). Elemental analysis calcd (%) for $C_9H_5O_8Tb$, [Tb(Htma)(H_2O)]: C 27.02, H 1.26 found: C 26.72, H 1.22.

3.3 Results and discussion

3.3.1 Synthesis and characterization

Eufda1 and **Tbfda1** have been successfully synthesized following a method described by Mooibroek *et al.*, which relies on the thermal decomposition of dmf to carbon monoxide and dimethylamine during reflux [19]. The dimethylamine thus formed facilitates the deprotonation of furan-2,5-dicarboxylic acid, allowing complex formation with the lanthanoid ion present.

The ligand H_4tma was readily obtained from 4-methylphenol following literature procedures to 2-methoxy-trimesic acid, followed by ether hydrolysis catalyzed by HBr, in satisfactory yield. Complex synthesis of terbium salts with this ligand via conventional methods failed to give pure compounds; hydrothermal synthesis methods appeared to give better results. Although the final compound has a metal to ligand ratio of 1:1, the use of a metal to ligand ratio of 1:3 in the hydrothermal complex synthesis was found to produce the desired compound in highest yields. It was found that a concentration of 10^{-2} M of Tb(III)

ions resulted in the formation of the largest crystals, being suitable for X-ray diffraction. Experiments using M:L ratios of 1:1 and 1:2 were found to give comparatively low yields of luminescent material, while Tb(III) concentrations in excess of $2 \cdot 10^{-2}$ M resulted in formation of microcrystalline materials. Formation of a complex is evidenced by the IR spectra of H_4tma and **TbHtma**; the absorption bands from the free-ligand carbonyl groups around 1660 cm^{-1} are shifted to 1580 cm^{-1} in the complex. The **TbHtma** was dried in a vacuum oven at 60 °C prior to elemental analysis, which resulted in driving off one mole of water from the compound.

3.3.2 X-ray crystal structure determination

A projection of part of the single crystal structure of **Eufda2** is shown in Figure 3.2; experimental crystallographic data are given in Table 3.1. The crystal structure determination reveals infinite Eu-fda chains, a single non-coordinating doubly deprotonated ligand molecule for every two lanthanoid ions and non-coordinated lattice water molecules. Two independent europium ions are present in the asymmetric unit; both europium ions are nine-coordinated. The coordination sphere of each lanthanoid ion contains four oxygen atoms from the carboxylate moiety of the ligand and is further saturated by coordination of five water molecules. The coordination geometry can be described as a distorted monocapped square antiprism, with a water molecule as top vertex, three water molecules and one carboxylato oxygen atom in the top square and a lower square comprising a single water molecule and three carboxylato oxygen atoms. The Eu-O distances are given in Table 3.2; they range from 2.378(2) to 2.580(2) Å, which are as expected [33]. Unlike the complexes with

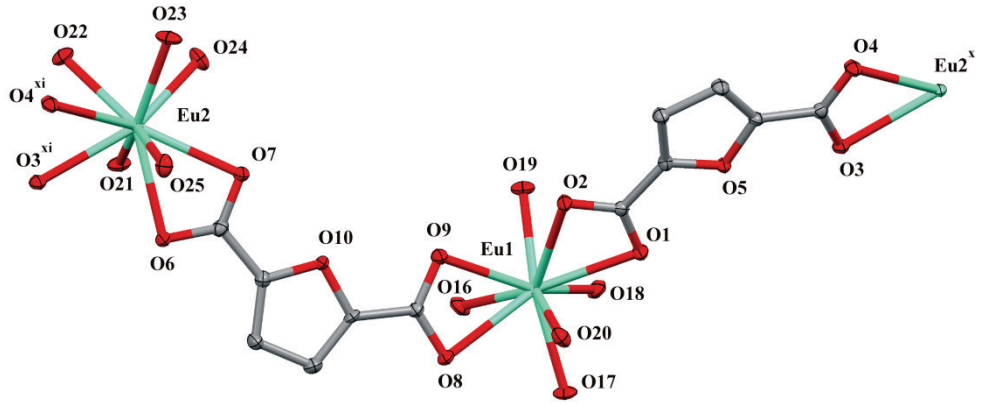

*Figure 3.2: projection of part of the crystal structure of **Eufda2**, showing the atom labeling scheme and the two Eu(III) sites. Atoms are shown as 50% displacement ellipsoids and hydrogen atoms are omitted for clarity. Symmetry operations: x (x, –1+y, 1+z); xi (x, 1+y, –1+z).*

pyridine-2,6-dicarboxylate and pyridine-2,6-dicarboxamide ligands reported before, the aromatic heteroatom is not coordinated to the lanthanoid. This is readily explained by the low basicity of the furan oxygen compared to the pyridine nitrogen. Perhaps the most striking feature is the presence of non-coordinating ligand molecules in the crystal structure. These ligands are stacked between the relatively flat Eu-fda chains and stabilize the crystal structure further by extensive hydrogen bonding involving nearby water molecules; hydrogen bond distances are given in Table 3.3. The coordinated ligand molecules also accept hydrogen bonds from non-coordinating water molecules, resulting in a 3-dimensional hydrogen bonding network. The presence of lattice water molecules is in agreement with the observation that the crystals rapidly decompose when removed from the mother liquor.

A projection of the crystal structure of **TbHtma** is given in Figure 3.3 and crystallographic data are summarized in Table 3.1. The asymmetric unit of **TbHtma** contains a single Tb(III) ion, one ligand and two molecules of water. The Tb ion has a coordination number of eight and the geometry around the Tb(III) ion can be described as a distorted biaugmented triangular prism. The two triangular faces of the prism are defined

Table 3.1: Details on the single crystal structure determination of complexes Eufda2 and TbHtma.

	Eufda2	**TbHtma**
formula	$C_{18}H_{38}Eu_2O_{31}$	$C_9H_7O_9Tb$
fw	1054.40	418.08
crystal size [mm^3]	0.56 × 0.13 × 0.05	0.02 × 0.04 × 0.28
crystal color	colorless	colorless
crystal system	triclinic	monoclinic
space group	$P\bar{1}$ (no. 2)	$P2_1/c$ (no.14)
a [Å]	10.7780(11)	9.402(1)
b [Å]	10.8948(11)	6.5399(5)
c [Å]	15.1161(15)	16.147(1)
α [°]	83.552(4)	90
β [°]	85.476(4)	110.95(1)
γ [°]	84.133(4)	90
V [$Å^3$]	1750.4(3)	927.2(2)
Z	2	4
d_{calc} [g/cm^3]	2.000	2.995
μ [mm^{-1}]	3.661	7.680
refl. measured / unique	51429 / 6461	13479 / 1636
parameters / restraints	460 / 0	193 / 3
R1/wR2 [I>2σ(I)]	0.0226 / 0.0569	0.0174 / 0.0424
R1/wR2 [all refl.]	0.0248 / 0.0585	0.0178 / 0.0427
S	1.111	1.17
$\rho_{min/max}$ [$e/Å^3$]	–1.05 / 2.08	–0.93 / 0.69

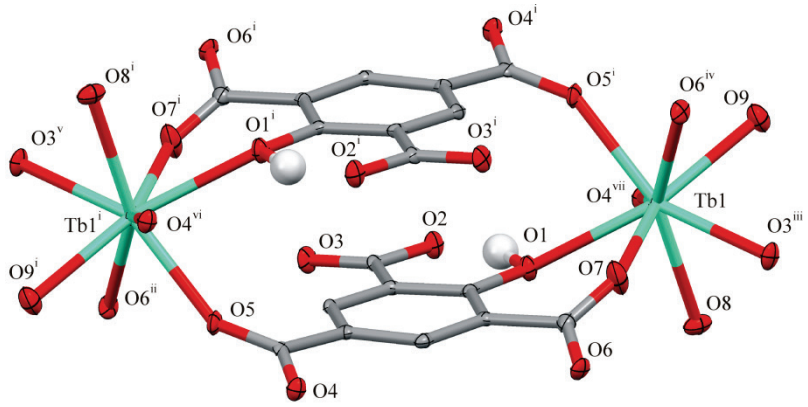

*Figure 3.3: Projection of part of the structure of **TbHtma** showing the labeling scheme and two sites for Tb(III). Atoms are shown as 30% displacement ellipsoids and hydrogen atoms except for H1 are omitted for clarity. Symmetry operations: i (2 – x, 1 – y, z); ii (x, 3/2 – y, – 1/2 + z); iii (x, 3/2 – y, 1/2 + z); iv (2 – x, – 1/2 + y, 1/2 – z); v (2 – x, – 1/2 + y, – 1/2 – z); vi (3 – x, 1 – y, – z); vii (– 1 + x, y, z).*

by (O1, O7, O8) and ($O5^{i}$, $O6^{iv}$, O9); the apexes of the square pyramids formed at two of the faces of this prism are defined by $O3^{iii}$ and $O4^{vii}$. Tb-O bond lengths are listed in Table 3.4; they range from 2.255(2) to 2.435(3) Å, which is normal for this type of bonds [18, 19, 33, 34]. Of interest is the mode of coordination of the ligand to the Tb(III) ion.The ligand provides four end-on bonds *via* its carboxylate groups and a bidentate chelating mode of bonding through the phenol oxygen and one of its neighboring carboxylate groups. The binding modes of the ligand in **TbHtma** are illustrated in Figure 3.4. Noteworthy is the strong intramolecular hydrogen bond between the phenolic proton and the carboxylate O2, with a H···O2 bond distance of 1.403(2) Å. No further hydrogen bonds can be identified in the structure.

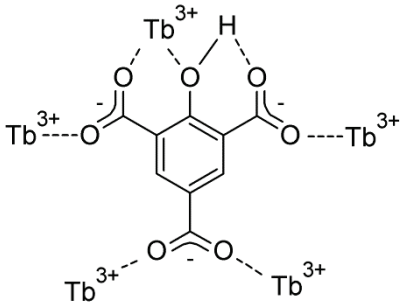

*Figure 3.4: schematic representation of the binding modes in **TbHtma**.*

The three dimensional structure of the network consists of puckered layers of ligand molecules, interacting by π-stacking with a perpendicular plane-to-plane distance of 3.265(1) Å, as is shown in Figure 3.5. The ligands of adjacent layers are connected by Tb(III) centers, and each Tb ion forms a node that connects five ligands, as is shown in Figure 3.6. All together, the three dimensional structure results in a highly dense packing with a calculated density as high as 2.995 g·cm^{-3}.

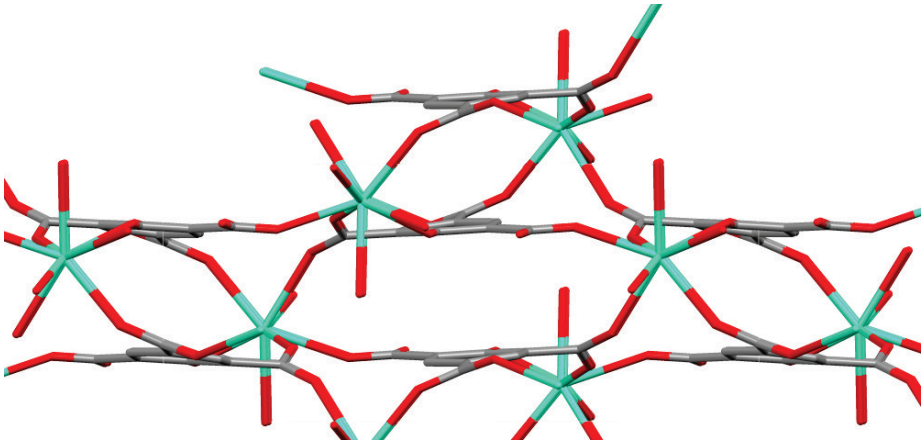

*Figure 3.5: Projection of the packing in **TbHtma** along the crystallographic a-axis, showing extensive pi-stacking in the structure.*

Table 3.2: selected bond distances (Å) and angles (°) for Eufda2. Atom labeling is shown in Figure 3.2.

Bond distance (Å)				Bond angle (°)	
Eu1-O1	2.483(2)	Eu2-O3	2.473(2)	O1-Eu1-O2	51.96(7)
Eu1-O2	2.544(2)	Eu2-O4	2.572(2)	O8-Eu1-O9	51.84(7)
Eu1-O8	2.580(2)	Eu2-O6	2.521(2)		
Eu1-O9	2.459(2)	Eu2-O7	2.499(2)		
Eu1-O16	2.409(2)	Eu2-O21	2.438(2)		
Eu1-O17	2.399(2)	Eu2-O22	2.413(2)		
Eu1-O18	2.434(2)	Eu2-O23	2.378(2)	O3-Eu2-O4	51.92(7)
Eu1-O19	2.442(2)	Eu2-O24	2.424(2)	O6-Eu2-O7	51.99(7)
Eu1-O20	2.417(2)	Eu2-O25	2.432(2)		

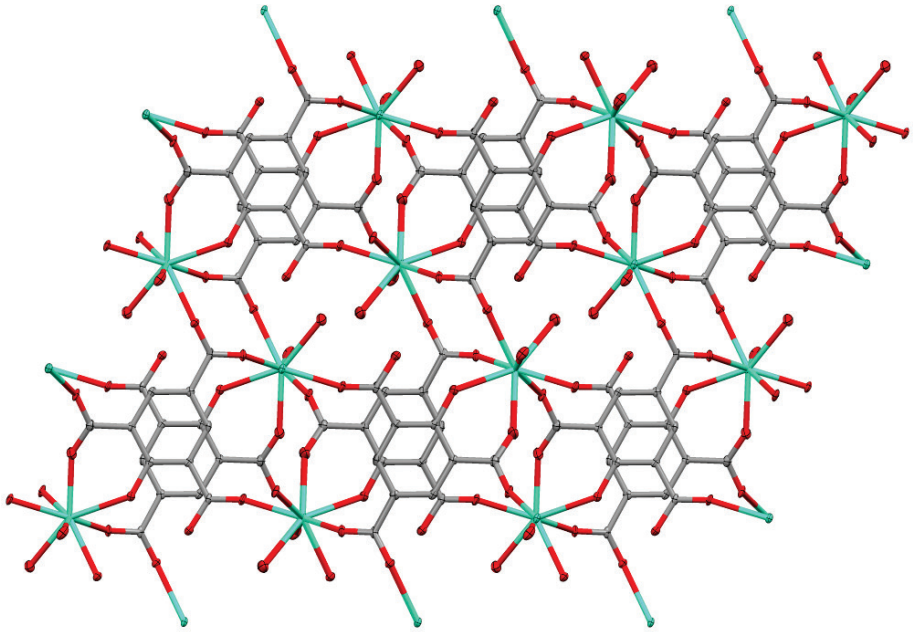

*Figure 3.6: A projection of the packing of **TbHtma** along the crystallographic y-axis, showing connectivity of the ligands and Tb(III) centers.*

Table 3.3: Hydrogen bonding geometries in Eufda2 with coordinated water as donor

D-H···A [Å]	D-H [Å]	H···A [Å]	D···A [Å]	D-H···A [°]
O16-H16A···O6^{i}	0.85	1.86	2.700(3)	173
O16-H16B···O5W^{ii}	0.92	1.85	2.759(3)	173
O17-H17A···O2W^{iii}	0.84	1.96	2.798(3)	175
O17-H17B···O3^{iv}	0.93	1.88	2.744(3)	154
O17-H17B···O5^{iv}	0.93	2.48	3.174(3)	131
O18-H18A···O1^{iv}	0.66	2.15	2.779(3)	160
O18-H18B···O3W^{ii}	0.95	1.83	2.763(3)	166
O19-H19A···O4W^{ii}	0.86	1.95	2.805(3)	172
O19-H19B···O4^{v}	0.80	1.98	2.781(3)	171
O20-H20A···O14^{i}	0.83	2.02	2.820(3)	162
O20-H20B···O14^{iii}	0.86	1.92	2.770(3)	169
O21-H21A···O8^{i}	0.74	2.02	2.728(3)	161
O21-H21B···O13	0.80	2.27	2.957(3)	144
O22-H22A···O1W^{vi}	0.81	2.00	2.783(3)	165
O22-H22B···O2^{vii}	0.92	1.77	2.688(3)	174
O23-H23A···O6W^{viii}	0.85	1.88	2.731(5)	177
O23-H23B···O9^{vii}	0.94	1.87	2.739(3)	153
O23-H23B···O10^{vii}	0.94	2.50	3.206(3)	132
O24-H24A···O7^{vii}	0.81	2.01	2.777(3)	160
O24-H24B···O11	0.85	1.94	2.781(3)	165
O25-H25A···O12^{ix}	0.88	1.87	2.730(3)	167
O25-H25B···O12^{vii}	0.88	1.99	2.805(4)	153

Symmetry operations: i (1 – x, 1 – y, 1 – z); ii (1 – x, – y, 1 – z); iii (x, y, z + 1); iv (1 – x, – y, 2 – z); v (2 – x, – y, 2 – z); vi (x + 1, y, z); vii (2 – x, 1 – y, 1 – z); viii (x + 1, y + 1, z); ix (x, y + 1, z).

Table 3.4: selected bond distances (Å) and angles (°) for TbHtma. Atom labeling is shown in Figure 3.3.

Bond distance		Bond angle	
Tb1-O1	2.403(3)	O3^{iii}-Tb1-O4^{vii}	121.40(9)
Tb1-O3^{iii}	2.287(2)	O5^{i}-Tb1-O6^{iv}	71.03(9)
Tb1-O4^{vii}	2.354(2)	O5^{i}-Tb1-O9	85.76(9)
Tb1-O5^{i}	2.255(2)	O6^{iv}-Tb1-O9	75.25(9)
Tb1-O6^{iv}	2.353(2)	O1-Tb1-O7	66.2(1)
Tb1-O7	2.274(3)	O1-Tb1-O8	79.38(9)
Tb1-O8	2.435(3)	O7-Tb1-O8	90.8(1)
Tb1-O9	2.336(3)		
Hydrogen bond			
O2···H1	1.403(2)		

Symmetry operations: i (2 – x, 1 – y, z); iii (x, 3/2 – y, 1/2 + z); iv (2 – x, – 1/2 + y, 1/2 – z); vii (– 1 + x, y, z).

3.3.3 Photoluminescence

*Complexes with the **fda** ligand*

The room temperature luminescence spectra were recorded for all four compounds, and are shown in Figure 3.7. All compounds exhibit luminescence spectra characteristic of the respective *Ln*(III) ions upon excitation in the ligand absorption band.

The emission spectrum of **Eufda1** shows lines at 591, 614, 651 and 698 nm, corresponding to the $^5D_0 \rightarrow {}^7F_1$, $^5D_0 \rightarrow {}^7F_2$ and $^5D_0 \rightarrow {}^7F_4$ transitions, respectively. The $^5D_0 \rightarrow {}^7F_1$ transition is a magnetic dipole (MD) transition and as such virtually insensitive to the crystal field around the Eu(III) ion, while the forced electric dipole (ED) transitions $^5D_0 \rightarrow {}^7F_2$ and $^5D_0 \rightarrow {}^7F_4$ are [35]. The fact that the $^5D_0 \rightarrow {}^7F_2$ ED transition is much stronger than the MD transition indicates a low symmetry Eu^{3+} site, lacking an inversion centre [36]. Apart from the lanthanoid-centered emission, a weak broad emission band around 450 nm is present. This feature is likely due to some residual ligand emission, resulting from incomplete energy transfer of the ligand to the lanthanoid ion. The excitation spectrum features two broad bands centered on 230 nm and 320 nm, which is typical for ligand-centered transitions. In addition, the strong line around 395 nm can be attributed to the ($^5L_6$, $^5G_2$, $^5L_7$, $^5G_3$) $\leftarrow {}^7F_0$ transitions of Eu^{3+} [37]. The emission spectrum of **Eufda2** shows features similar to that of the **Eufda1** compound, with no significant shift of the emission lines. The broad ligand-centered emission is completely absent, indicating more complete ligand to lanthanoid energy transfer. Judged by the naked eye, the luminescence intensity of **Eufda2** is weak compared to **Eufda1** upon excitation by a standard UV lamp at 254 nm.

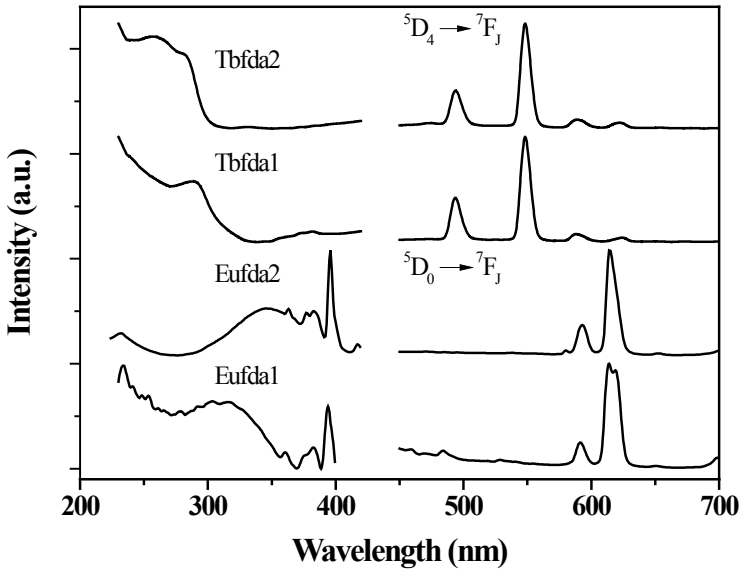

*Figure 3.7: From bottom to top: excitation (left) and emission (right) spectra for **Eufda1**, **Eufda2**, **Tbfda1** and **Tbfda2** recorded at room temperature in the solid state. The emission spectra are characteristic of the lanthanoid ion.*

This difference in intensity could not be quantified due to limitations of the equipment used to record the spectra. The excitation spectrum features a broad band around 340 nm that corresponds to a ligand-centered transition, and again a strong line around 395 nm due to direct excitation into the Eu^{3+} 4f manifold. Compared to the excitation spectrum of **Eufda1**, the excitation band of **Eufda2** is shifted to longer wavelengths, which is likely due to structural differences between **Eufda1** and **Eufda2**. Because of the forbidden nature of the 4f – 4f transitions, direct excitation into the 4f manifold is inefficient. Yet the intensity of this line is higher than the ligand-centered excitation band, indicating that ligand centered excitation is comparatively weak. When excited in the ligand-centered excitation band, the complex **Tbfda1** exhibits luminescence characteristic of Tb(III), with sharp lines at 494, 549, 589, and 624 nm. These are readily assigned to transitions from the $^5D_4$-state to $^7F_6$, $^7F_5$, $^7F_4$ and $^7F_3$ states, respectively. The excitation spectrum shows a broad band with a maximum at 289 nm, originating from the ligand centered $\pi^* \leftarrow \pi$ transition. This band extends to 320 nm, making it blue shifted compared to the excitation spectrum of **Eufda1**. In addition, a very weak band between 350 and 400 nm can be observed, resulting from excitations from the $^7F_6$ state to the $^5D_3$, $^5G_6$, $^5L_{10}$, $^5G_5$, $^5D_2$, $^5G_4$ and $^5L_9$ levels [37]. Comparing the **Tbfda2** emission spectrum with the one obtained for **Tbfda1**, no significant shift can be observed in the emission lines. The luminescence intensity of **Tbfda2** is weak compared to **Tbfda1** upon excitation by a standard UV lamp at 254 nm, as judged by the

eye. The excitation spectrum is somewhat blue shifted, featuring a single broad band with a maximum around 256 nm.
The furan-dicarboxylate ligand thus appears to be able to sensitize both Eu(III) and Tb(III) centered luminescence. The typical sensitization mechanism involves excitation of the ligand to an excited singlet state, S* ← S, followed by intersystem crossing to a triplet state S* → T* which is promoted by the heavy atom effect due to the lanthanoid ion. Subsequently, energy transfer from ligand to lanthanoid occurs, which is followed by lanthanoid-centered emission [38]. To avoid thermal repopulation of the ligand's triplet state, it must be at least 1,850 cm^{-1} higher in energy than the emissive level of the lanthanoid ion [39]. For Tb(III) complexes, this suggests a triplet state of at least 22,350 cm^{-1}, whereas for Eu(III) complexes the energetic requirements are less clear cut because of its multiple acceptor levels [40].
In both **Eufda2** and **Tbfda2**, the lanthanoid ion is surrounded by five molecules of water. It is known that water molecules present in the first coordination sphere of a lanthanoid ion are efficient luminescence quenchers [41, 42]. This is a result of energy transfer from the lanthanoid ion's excited state to O-H oscillators provided by the coordinated water molecules. Although the coordinated water does not fully quench the luminescence of the lanthanoid ion, it most certainly lowers both luminescence lifetime and intensity of **Eufda2** and **Tbfda2**. This may explain why **Eufda2** and **Tbfda2** give relatively weak luminescence compared to **Eufda1** and **Tbfda1**, respectively.

*Complex with the **Htma** ligand*

Upon illumination of **TbHtma** by a standard laboratory UV lamp emitting at 366 nm, the compound exhibits bright green emission. Photoluminescence spectra recorded in the solid-state for **TbHtma** are shown in Figure 3.8. The excitation spectrum shows a broad band in the nUV region with a maximum at 378 nm, which is typical for ligand-centered excitation. The emission spectrum is characteristic of the Tb(III)-ion, with transitions from the $^5D_4$ level to the ^7F_J manifold appearing as emission lines at 492 nm ($J = 6$), 549 nm ($J = 5$), 588 nm ($J = 4$) and 622 nm ($J = 3$). The $^5D_4 \rightarrow {}^7F_5$ transition dominates the emission spectrum, contributing over 70% to the total emission intensity. The emission lines are visibly split as a result of crystal field splitting. The photoluminescence quantum yield determined for this compound is 67% upon excitation at 380 nm. This is a remarkably high value, even higher than the value reported for the Tb(III) complex with 5-*tert*-butyl-2-hydroxy-isophthalate as a ligand (52%) or the Tb(III) complexes with 2-hydroxyphthalimide ligands (59 and 61%) [43, 44]. The luminescence decay curve is shown in Figure 3.9, and a single exponential function was fitted to it, yielding a lifetime of 0.50 ms. This is as expected for a Tb(III) compound with a single luminescent center.

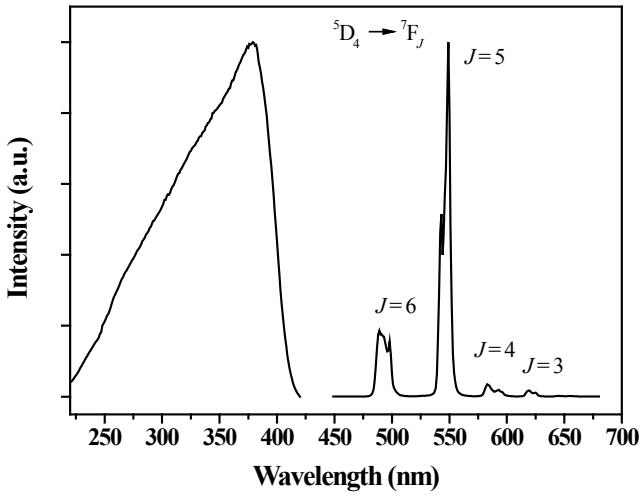

*Figure 3.8: Excitation (left, λ_{em} = 549 nm) and emission (right, λ_{exc} = 360 nm) spectra recorded for **TbHtma** in the solid state at room temperature. The emission spectrum is characteristic for the Tb(III) ion.*

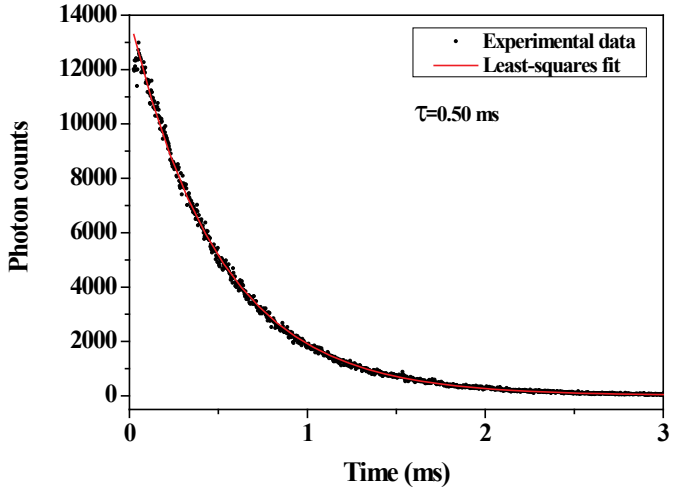

*Figure 3.9: The luminescence decay curve obtained for **TbHtma** in the solid state at room temperature (black line) and the least squares fit of a single-exponential decay-curve (red line).*

3.4 Conclusion

Four new Eu(III) and Tb(III) complexes have been synthesized using the furan-2,5-dicarboxylate ligand. Synthesis in dmf provides the anhydrous compounds described by the general formula $(H_2NMe_2)_6Ln_4Cl_4(fda)_7$ (*Ln* = Eu, Tb). Both compounds exhibit luminescence characteristic of the lanthanoid upon ligand centered excitation,

showing that in both cases the ligand acts as an antenna. Due to their low efficiency, neither compound is suitable for application as a phosphor material in LEDs. Recrystallisation from water results in the formation of $([Ln(fda)\cdot(H_2O)_5]\cdot\frac{1}{2}(fda)\cdot 3H_2O)_n$ (*Ln* = Eu, Tb) that also show lanthanoid-centered emission. The crystal structure of the latter compound reveals two low-symmetry *Ln*-sites, which is consistent with the luminescence spectra. 2-Hydroxy-trimesic acid has been synthesized from 4-methylphenol using standard literature procedures in non-optimized yields. It has been reacted with $TbCl_3$ under hydrothermal conditions, giving a novel metal-organic framework type compound with the formula $[Tb(Htma)(H_2O)_2]$. This compound exhibits very efficient photoluminescence characteristic for the Tb(III)-ion upon excitation of the ligand-centered absorption band by near-UV radiation. The quantum yield for this process is 67%, indicating that 2-hydroxytrimesic acid is a highly efficient antenna for the sensitization of Tb(III) emission. Owing to its high quantum yield and long excitation wavelength, this compound is an ideal candidate green phosphor material for application in LEDs.

3.5 References

[1] J.M. Phillips, M.E. Coltrin, M.H. Crawford, A.J. Fischer, M.R. Krames, R. Mueller-Mach, G.O. Mueller, Y. Ohno, L.E.S. Rohwer, J.A. Simmons, and J.Y. Tsao, *Laser Photonics Rev.*, 1 (2007) 307-333.

[2] R.-J. Xie and N. Hirosaki, *Sci. Technol. Adv. Mat.*, 8 (2007) 588-600.

[3] H.A. Höppe, *Angew. Chem., Int. Ed.*, 48 (2009) 3572-3582.

[4] A.A. Setlur, *Electrochem. Soc. Interface*, 18 (2009) 32-36.

[5] C.C. Lin and R.-S. Liu, *J. Phys. Chem. Lett.*, 2 (2011) 1268-1277.

[6] S.I. Weissman, *J. Chem. Phys.*, 10 (1942) 214-217.

[7] R.E. Whan and G.A. Crosby, *J. Mol. Spectrosc.*, 8 (1962) 315-327.

[8] K. Binnemans, *Chem. Rev.*, 109 (2009) 4283-4374.

[9] P. He, H.H. Wang, S.G. Liu, J.X. Shi, G. Wang, and M.L. Gong, *Inorg. Chem.*, 48 (2009) 11382-11387.

[10] C.R. De Silva, J.R. Maeyer, R. Wang, G.S. Nichol, and Z. Zheng, *Inorg. Chim. Acta*, 360 (2007) 3543-3552.

[11] R.D. Archer, H. Chen, and L.C. Thompson, *Inorg. Chem.*, 37 (1998) 2089-2095.

[12] H. Chen and R.D. Archer, *Inorg. Chem.*, 33 (1994) 5195-5202.

[13] D. Parker, P.K. Senanayake, and J.A.G. Williams, *J. Chem. Soc., Perkin Trans. 2*, (1998) 2129-2140.

[14] J.-C.G. Bünzli, *J. Alloys Compd.*, 408-412 (2006) 934-944.

[15] V. Tsaryuk, K. Zhuravlev, V. Zolin, P. Gawryszewska, J. Legendziewicz, V. Kudryashova, and I. Pekareva, *J. Photochem. Photobiol., A*, 177 (2006) 314-323.

[16] K. Liu, G. Jia, Y. Zheng, Y. Song, M. Yang, Y. Huang, L. Zhang, and H. You, *Inorg. Chem. Commun.*, 12 (2009) 1246-1249.

[17] T. Zhu, K. Ikarashi, T. Ishigaki, K. Uematsu, K. Toda, H. Okawa, and M. Sato, *Inorg. Chim. Acta*, 362 (2009) 3407-3414.

[18] S. Tanase, P.M. Gallego, R. de Gelder, and W.T. Fu, *Inorg. Chim. Acta*, 360 (2007) 102-108.

[19] T.J. Mooibroek, P. Gamez, A. Pevec, M. Kasunič, B. Kozlevčar, W.T. Fu, and J. Reedijk, *Dalton Trans.*, 39 (2010) 6483-6487.
[20] J.C. de Mello, H.F. Wittmann, and R.H. Friend, *Adv. Mater.*, 9 (1997) 230-232.
[21] Bruker, *SAINT-plus*, 2001. Bruker AXS Inc: Madison, Wisconsin, USA. p.
[22] G.M. Sheldrick, *SADABS: Area-Detector Absorption Correction*, 1999. Universität Göttingen: Göttingen, Germany. p.
[23] P.T. Beurskens, G. Beurskens, R. de Gelder, S. Garcia-Granda, R.O. Gould, and J.M.M. Smits, *The DIRDIF2008 program system*, 2008. Crystallography Laboratory, University of Nijmegen: Nijmegen, The Netherlands. p.
[24] G.M. Sheldrick, *Acta Crystallogr., Sect. A: Found. Crystallogr.*, 64 (2008) 112-122.
[25] A.L. Spek, *Acta Crystallogr., Sect. D: Biol. Crystallogr.*, 65 (2009) 148-155.
[26] T. Kottke and D. Stalke, *J. Appl. Crystallogr.*, 26 (1993) 615-619.
[27] G.M. Sheldrick, *SHELXS–97*, *Bruker AXS Inc., Madison, Wisconsin*, 1997.
[28] Nonius, *COLLECT*, *Nonius BV, Delft, The Netherlands*, 2002.
[29] F. Ullmann and K. Brittner, *Ber. Dtsch. Chem. Ges.*, 42 (1909) 2539-2548.
[30] H.T. Openshaw and R. Robinson, *J. Chem. Soc.*, (1946) 912-918.
[31] R. Gupta, S. Mukherjee, and R. Mukherjee, *J. Chem. Soc., Dalton Trans.*, (1999) 4025-4030.
[32] K.N. Raymond, S. Petoud, and J. Xu, Aromatic Triamide-Lanthanide Complexes, Pat.no 20090036537, 2009.
[33] A.G. Orpen, L. Brammer, F.H. Allen, O. Kennard, D.G. Watson, and R. Taylor, *J. Chem. Soc., Dalton Trans.*, (1989) S1-S83.
[34] X.-Q. Zhao, B. Zhao, S. Wei, and P. Cheng, *Inorg. Chem.*, 48 (2009) 11048-11057.
[35] C. Görller-Walrand and K. Binnemans, *Spectral intensities of f-f transitions*, in *Handbook on the Physics and Chemistry of Rare Earths*, 1998, Elsevier. 99-264.
[36] R. Reisfeld, E. Zigansky, and M. Gaft, *Mol. Phys.*, 102 (2004) 1319 - 1330.
[37] W.T. Carnall, P.R. Fields, and K. Rajnak, *J. Chem. Phys.*, 49 (1968) 4412-4423.
[38] W.F. Sager, N. Filipescu, and F.A. Serafin, *J. Phys. Chem.*, 69 (1965) 1092-1100.
[39] M. Latva, H. Takalo, V.M. Mukkala, C. Matachescu, J.C. Rodriguez-Ubis, and J. Kankare, *J. Lumin.*, 75 (1997) 149-169.
[40] W.T. Carnall, P.R. Fields, and K. Rajnak, *J. Chem. Phys.*, 49 (1968) 4447-4449.
[41] S. Meshkova, Z. Topilova, M. Lozinskii, and D. Bol'shoi, *J. Appl. Spectrosc.*, 64 (1997) 229-233.
[42] Y. Hasegawa, Y. Wada, and S. Yanagida, *J. Photochem. Photobiol., C*, 5 (2004) 183-202.
[43] L. Benisvy, P. Gamez, W.T. Fu, H. Kooijman, A.L. Spek, A. Meijerink, and J. Reedijk, *Dalton Trans.*, (2008) 3147-3149.
[44] S. Petoud, S.M. Cohen, J.-C.G. Bünzli, and K.N. Raymond, *J. Am. Chem. Soc.*, 125 (2003) 13324-13325.